

Supplementary Information

Hierarchical Chirality Transfer of Perylene Diimide-tethered Pillar[5]arenes for Configuration and Type Differentiation of Amino Acid Derivatives

Ting Zhao, Jigao Yi, Chunhong Liu, Lizhi Fang, Long Chen, Yanlin Shen, Xiaotong Liang,
Kun Li, Wanhua Wu^[a] and Cheng Yang*^[a]

Key Laboratory of Green Chemistry & Technology of Ministry of Education, College of Chemistry Institution, Sichuan University
Chengdu 610064 (China)
E-mail: yangchengyc@scu.edu.cn

Materials and Instruments

L- and D-amino acid alkyl ester hydrochlorides enantiomers (99%) were purchased from Sigma Aldrich. All chemicals and solvents were used as received without further purification. ^1H NMR spectra were recorded at room temperature on Bruker AMX-400 (operating at 400 MHz for ^1H NMR) and all chemical shifts are reported in ppm with TMS as the internal standard. UV-vis spectra were obtained on a JASCO V650 spectrometer at room temperature. Fluorescence spectra were taken on Fluoromax-4 spectrofluorometer. Circular dichroism (CD) spectra were recorded on a JASCO J-1500 spectrometer using a quartz cuvette of 1 cm path length.

S1, C8 and amino acid derivatives were synthesized according to the previously reported methods.

1

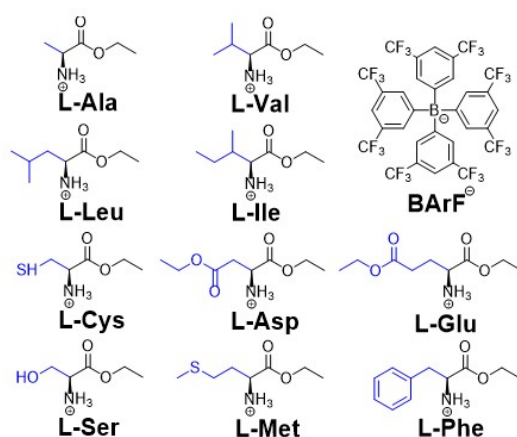


Fig. S1. Chemical structures of amino acid derivatives.

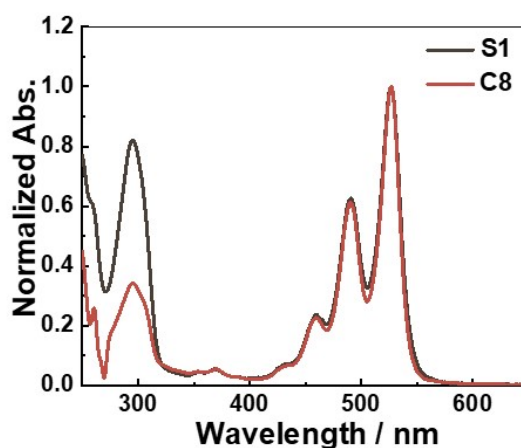


Fig. S2. Normalized UV-Vis absorption spectra of S1 and C8 in CHCl_3 .

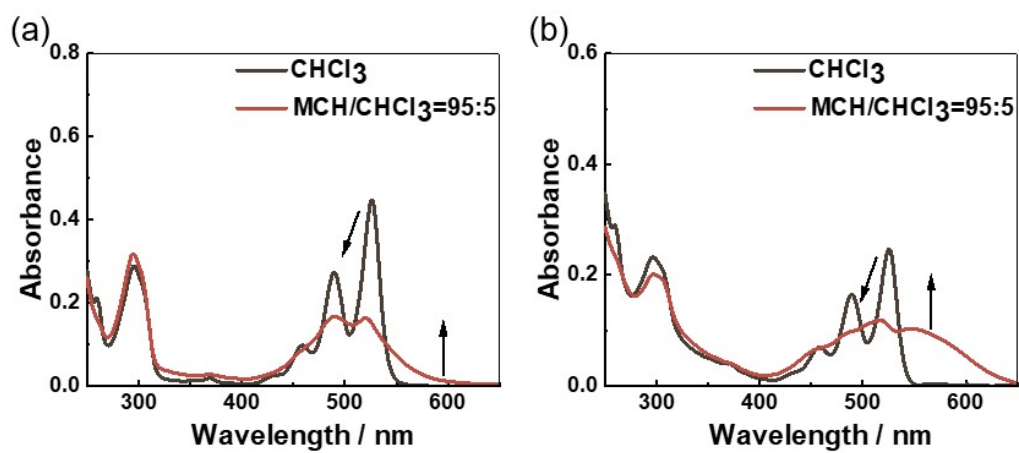


Fig. S3. Solvent-dependent UV-Vis absorption spectra of (a) S1 (0.01 mM), (b) C8 (0.01 mM) from pure CHCl_3 to 95% MCH.

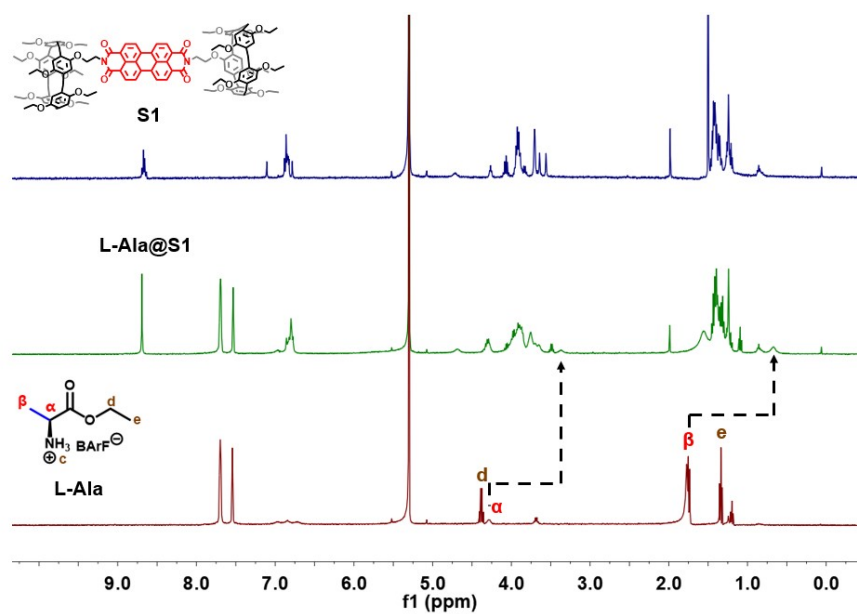


Fig. S4. ^1H NMR spectra (400 MHz, CD_2Cl_2 , 298 K) of S1 (1 mM) (blue), L-Ala@S1 ($[\text{L-Ala}] = 2 \text{ mM}$, $[\text{L-Ala}]/[\text{S1}] = 2$) (green) and L-Ala (1 mM) (red).

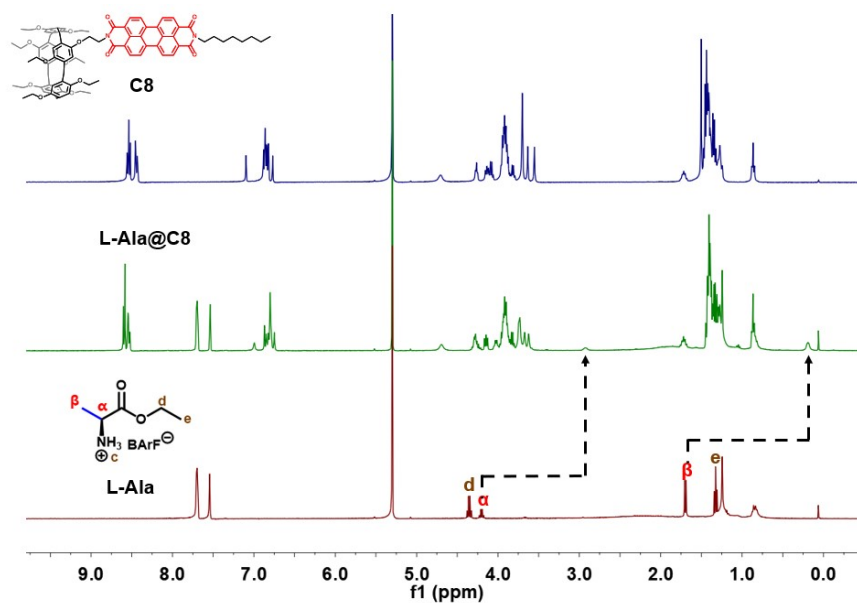


Fig. S5. ^1H NMR spectra (400 MHz, CD_2Cl_2 , 298 K) of **C8** (1 mM) (blue), L-Ala@**C8** ([L-Ala] = [C8] = 1 mM) (green) and L-Ala (1 mM) (red).

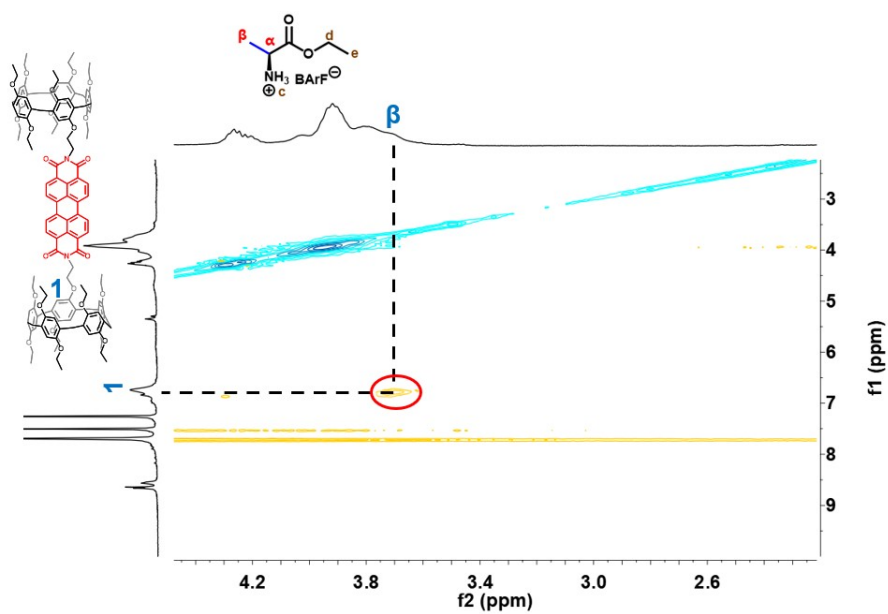


Fig. S6. ^1H - ^1H ROESY NMR (400 MHz, CDCl_3 , 298 K) spectra of L-Ala@**S1** ([L-Ala] = 2 mM, [L-Ala]/[S1] = 2).

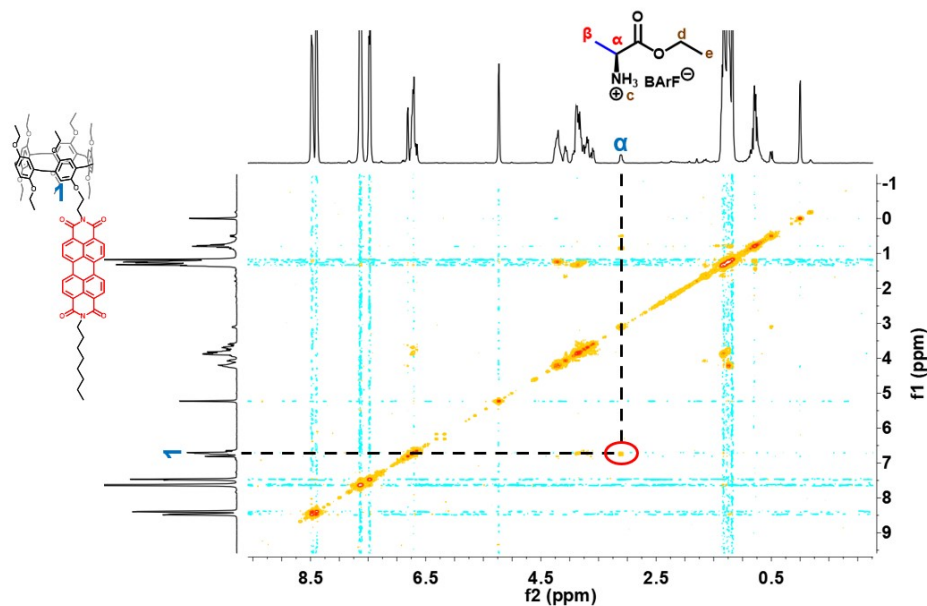


Fig. S7. ^1H - ^1H ROESY NMR (400 MHz, CD_2Cl_2 , 298 K) spectra of L-Ala@C8 ([L-Ala] = [C8] = 1 mM).

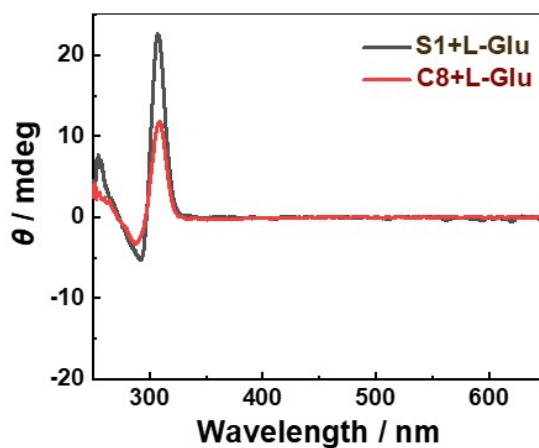


Fig. S8. CD spectra of S1 (0.05 mM) and C8 (0.05 mM) with L-Glu (100 μM) in CHCl_3 at 25 $^\circ\text{C}$.

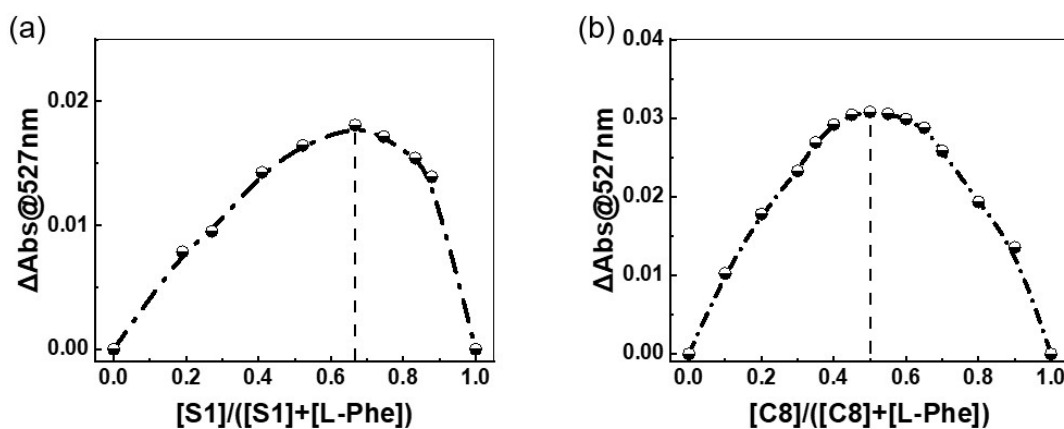


Fig. S9. Job's plot based on the intensity changes at 527 nm in the UV-vis absorption spectra in CHCl_3 (25 $^\circ\text{C}$) for the complexation of L-Phe with (a) S1 and (b) C8. $[\text{G}] + [\text{H}] = 0.05 \text{ mM}$.

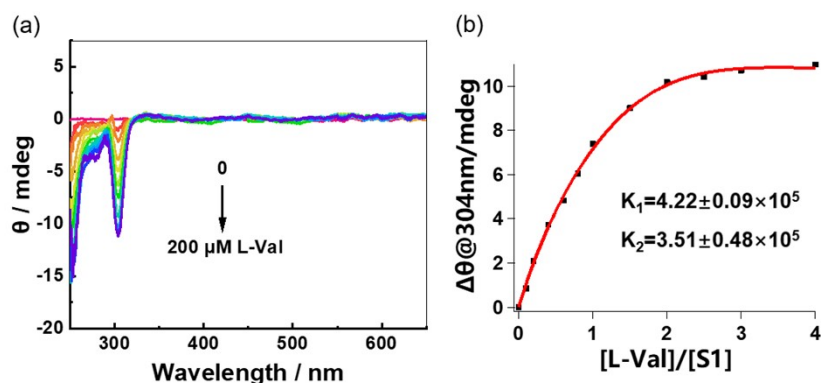


Fig. S10. (a) CD spectra of **S1** (0.05 mM) upon titration with L-Val (0-200 μM) in CHCl_3 at 25 $^\circ\text{C}$. (b) The non-linear curve-fitting based on the CD intensity changes at 304 nm, from which the association constants (K) for the formation of the 1:2 complexes were estimated to be $K_1 = 4.22 \pm 0.09 \times 10^5 \text{ M}^{-1}$ and $K_2 = 3.51 \pm 0.48 \times 10^5 \text{ M}^{-1}$, respectively.

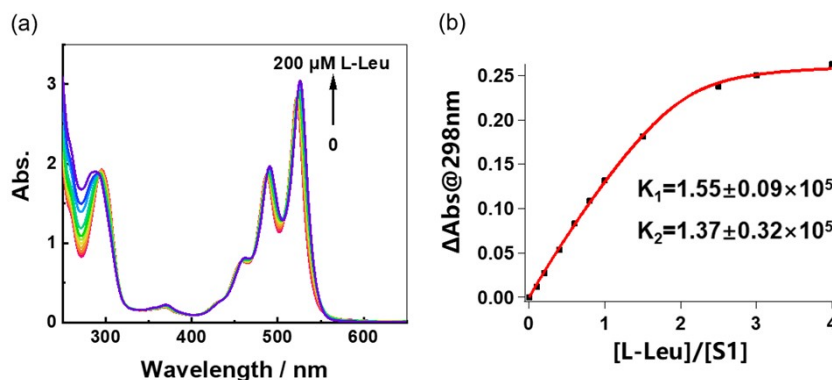


Fig. S11. (a) UV-Vis spectra of **S1** (0.05 mM) upon titration with L-Leu (0-200 μM) in CHCl_3 at 25 $^\circ\text{C}$. (b) The non-linear curve-fitting based on the UV-Vis intensity changes at 298 nm, from which the association constants (K) for the formation of the 1:2 complexes were estimated to be $K_1 = 1.55 \pm 0.09 \times 10^5 \text{ M}^{-1}$ and $K_2 = 1.37 \pm 0.32 \times 10^5 \text{ M}^{-1}$, respectively.

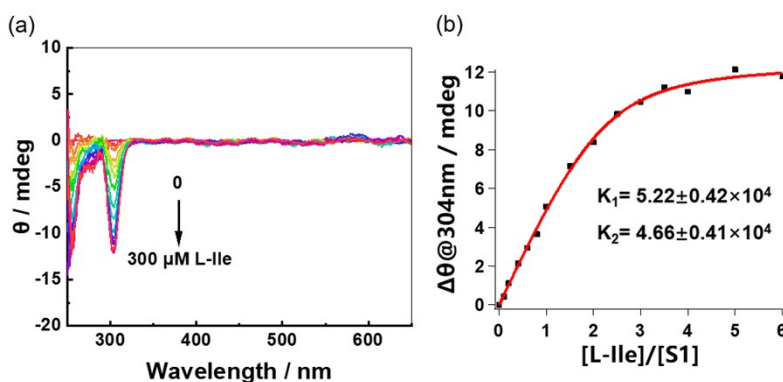


Fig. S12. (a) CD spectra of **S1** (0.05 mM) upon titration with L-Ile (0-300 μM) in CHCl_3 at 25 $^\circ\text{C}$. (b) The non-linear curve-fitting based on the CD intensity changes at 304 nm, from which the association constants (K) for the formation of the 1:2 complexes were estimated to be $K_1 = 5.22 \pm 0.42 \times 10^4 \text{ M}^{-1}$ and $K_2 = 4.66 \pm 0.41 \times 10^4 \text{ M}^{-1}$,

respectively.

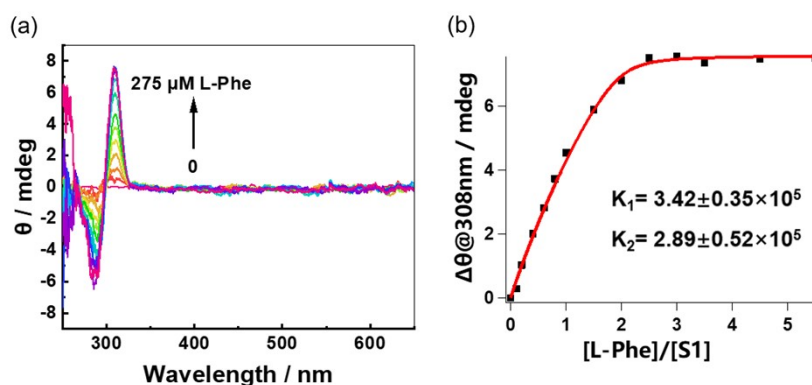


Fig. S13. (a) CD spectra of **S1** (0.05 mM) upon titration with L-Phe (0-275 μM) in CHCl_3 at 25 $^\circ\text{C}$. (b) The non-linear curve-fitting based on the CD intensity changes at 308 nm, from which the association constants (K) for the formation of the 1:2 complexes were estimated to be $K_1 = 3.42 \pm 0.35 \times 10^5 \text{ M}^{-1}$ and $K_2 = 2.89 \pm 0.52 \times 10^5 \text{ M}^{-1}$, respectively.

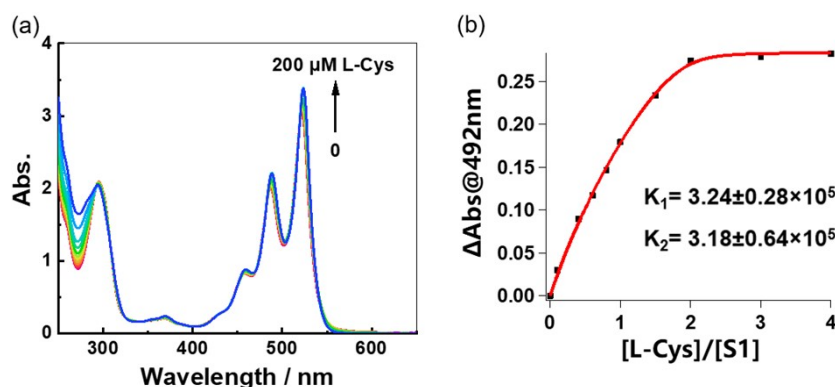


Fig. S14. (a) UV-Vis spectra of **S1** (0.05 mM) upon titration with L-Cys (0-200 μM) in CHCl_3 at 25 $^\circ\text{C}$. (b) The non-linear curve-fitting based on the UV-Vis intensity changes at 492 nm, from which the association constants (K) for the formation of the 1:2 complexes were estimated to be $K_1 = 3.24 \pm 0.28 \times 10^5 \text{ M}^{-1}$ and $K_2 = 3.18 \pm 0.64 \times 10^5 \text{ M}^{-1}$, respectively.

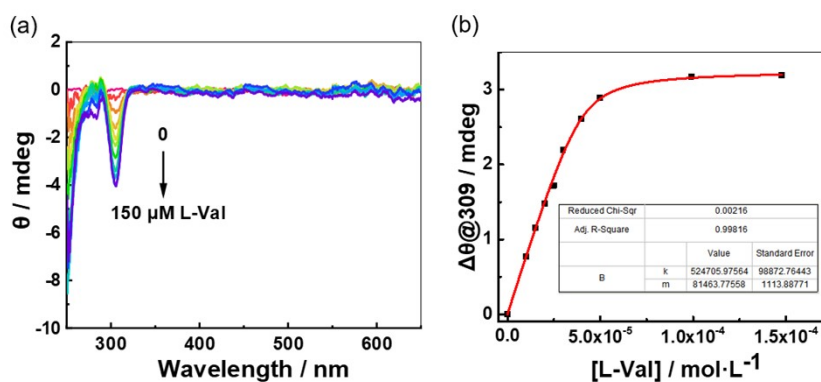


Fig. S15. (a) CD spectra of **C8** (0.05 mM) upon titration with L-Val (0-150 μM) in CHCl_3 at 25 $^\circ\text{C}$. (b) The non-linear curve-fitting based on the CD intensity changes at 309 nm, from which the association constants (K) for the formation of the 1:1 complexes were estimated to be $K = 5.25 \pm 0.99 \times 10^5 \text{ M}^{-1}$.

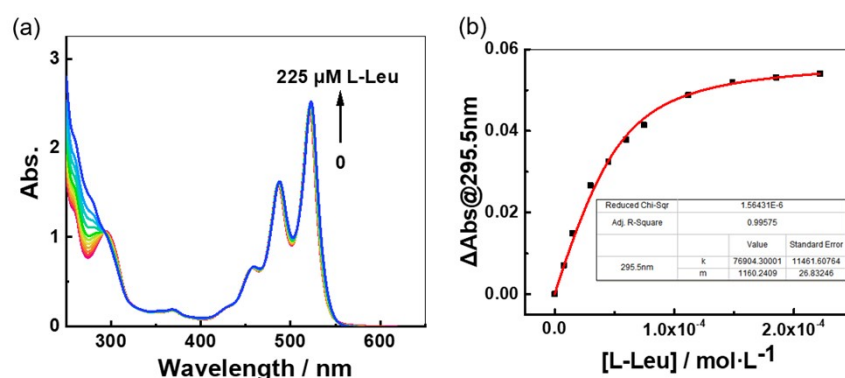


Fig. S16. (a) UV-Vis spectra of **C8** (0.05 mM) upon titration with L-Leu (0-225 μM) in CHCl_3 at 25 $^\circ\text{C}$. (b) The non-linear curve-fitting based on the UV-Vis intensity changes at 295.5 nm, from which the association constants (K) for the formation of the 1:1 complexes were estimated to be $K = 7.69 \pm 1.12 \times 10^4 \text{ M}^{-1}$.

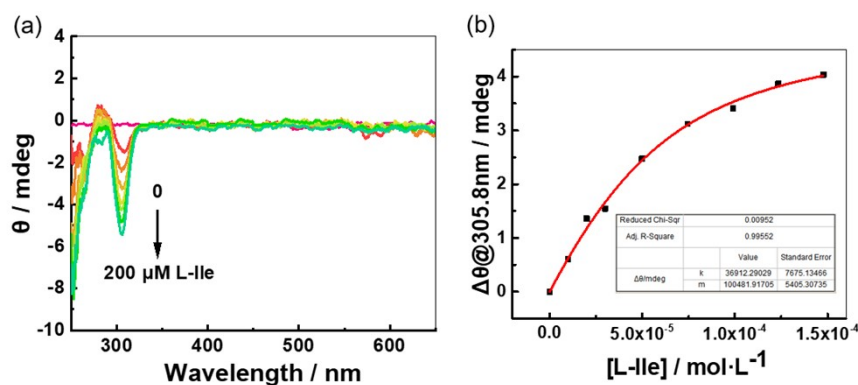


Fig. S17. (a) CD spectra of **C8** (0.05 mM) upon titration with L-Ile (0-200 μM) in CHCl_3 at 25 $^\circ\text{C}$. (b) The non-linear curve-fitting based on the CD intensity changes at 305.8 nm, from which the association constants (K) for the formation of the 1:1 complexes were estimated to be $K = 3.69 \pm 0.77 \times 10^4 \text{ M}^{-1}$.

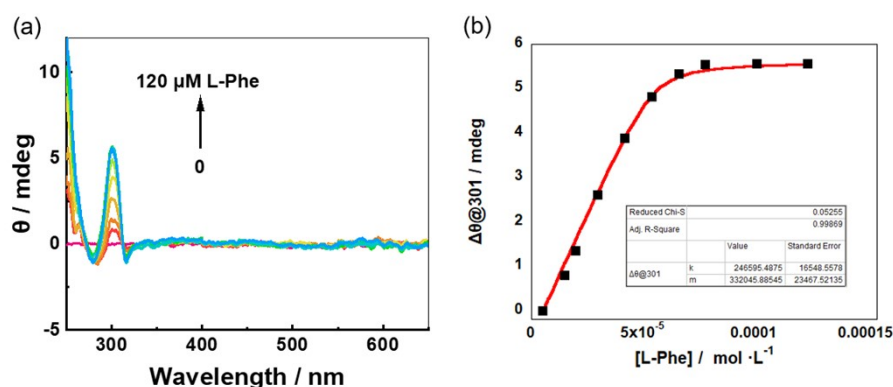


Fig. S18. (a) CD spectra of **C8** (0.05 mM) upon titration with L-Phe (0-120 μM) in CHCl_3 at 25 $^\circ\text{C}$. (b) The non-linear curve-fitting based on the CD intensity changes at 301 nm, from which the association constants (K) for the formation of the 1:1 complexes were estimated to be $K = 2.47 \pm 0.16 \times 10^5 \text{ M}^{-1}$.

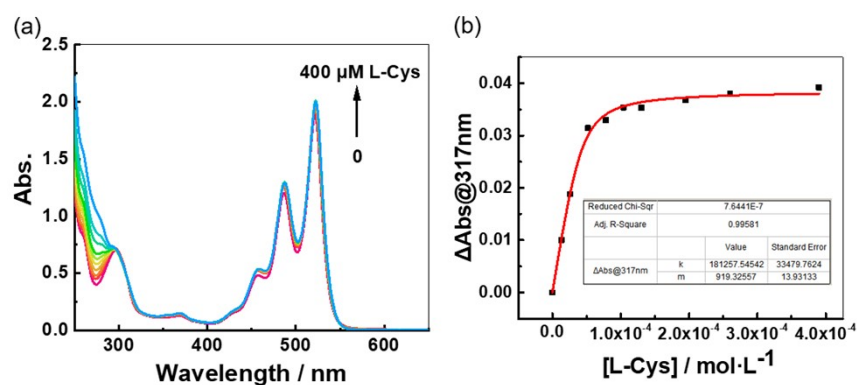


Fig. S19. (a) UV-Vis spectra of **C8** (0.05 mM) upon titration with L-Cys (0-400 μM) in CHCl_3 at 25 $^\circ\text{C}$. (b) The non-linear curve-fitting based on the UV-Vis intensity changes at 317 nm, from which the association constants (K) for the formation of the 1:1 complexes were estimated to be $K = 1.81 \pm 0.33 \times 10^5 \text{ M}^{-1}$.

Table S1. Binding constants (K , M^{-1}) for **S1** and **C8** with amino acid derivatives.

	S1		C8
	K_1 (M^{-1})	K_2 (M^{-1})	K (M^{-1})
L-Ala ^a	$2.73 \pm 0.33 \times 10^5$	$2.74 \pm 0.62 \times 10^5$	$2.07 \pm 0.33 \times 10^5$
L-Val	$4.22 \pm 0.09 \times 10^5$	$3.51 \pm 0.48 \times 10^5$	$5.25 \pm 0.99 \times 10^5$
L-Leu	$1.55 \pm 0.09 \times 10^5$	$1.37 \pm 0.32 \times 10^5$	$7.69 \pm 1.12 \times 10^4$
L-Ile	$5.22 \pm 0.42 \times 10^4$	$4.66 \pm 0.41 \times 10^4$	$3.69 \pm 0.77 \times 10^4$
L-Phe	$3.42 \pm 0.35 \times 10^5$	$2.89 \pm 0.52 \times 10^5$	$2.47 \pm 0.16 \times 10^5$
L-Asp	$7.57 \pm 0.25 \times 10^4$	$7.65 \pm 0.37 \times 10^4$	$8.89 \pm 1.60 \times 10^4$
L-Glu ^a	$7.00 \pm 0.61 \times 10^5$	$7.01 \pm 1.20 \times 10^5$	$3.23 \pm 0.28 \times 10^5$
L-Ser ^a	$7.67 \pm 0.11 \times 10^5$	$7.70 \pm 0.13 \times 10^5$	$6.41 \pm 0.91 \times 10^5$
L-Met ^a	$9.35 \pm 0.51 \times 10^3$	$6.06 \pm 0.72 \times 10^3$	$7.64 \pm 1.06 \times 10^3$
L-Cys	$3.24 \pm 0.28 \times 10^5$	$3.18 \pm 0.64 \times 10^5$	$1.81 \pm 0.33 \times 10^5$

The K (K_1 and K_2 where two values are listed) were obtained from CD or UV-vis spectroscopic titrations with $[\text{S1}] = [\text{C8}] = 0.05 \text{ mM}$ in CHCl_3 at 25 $^\circ\text{C}$. ^a K value from previous work. ^{1a}

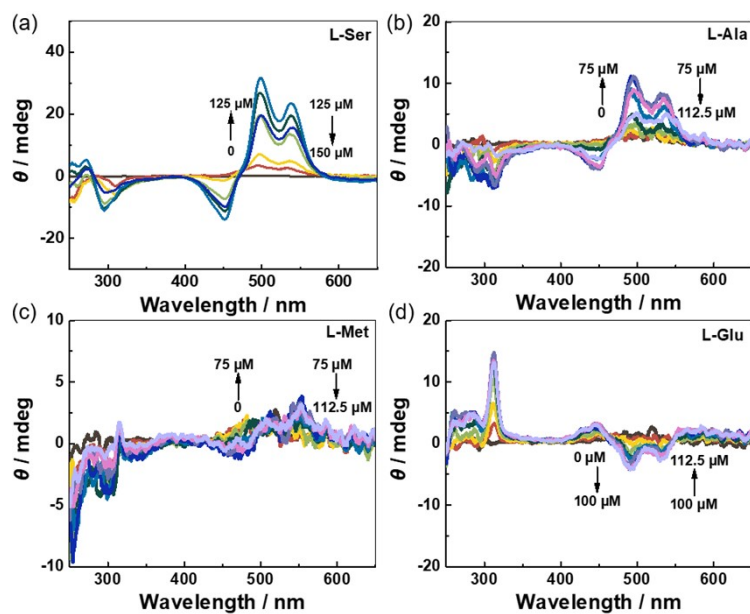


Fig. S20. CD spectra of S1 (0.05 mM) upon titration with (a) L-Ser (0-150 μ M), (b) L-Ala (0-112.5 μ M), (c) L-Met (0-112.5 μ M), (d) L-Glu (0-112.5 μ M) in 95% MCH at 25 $^{\circ}$ C.

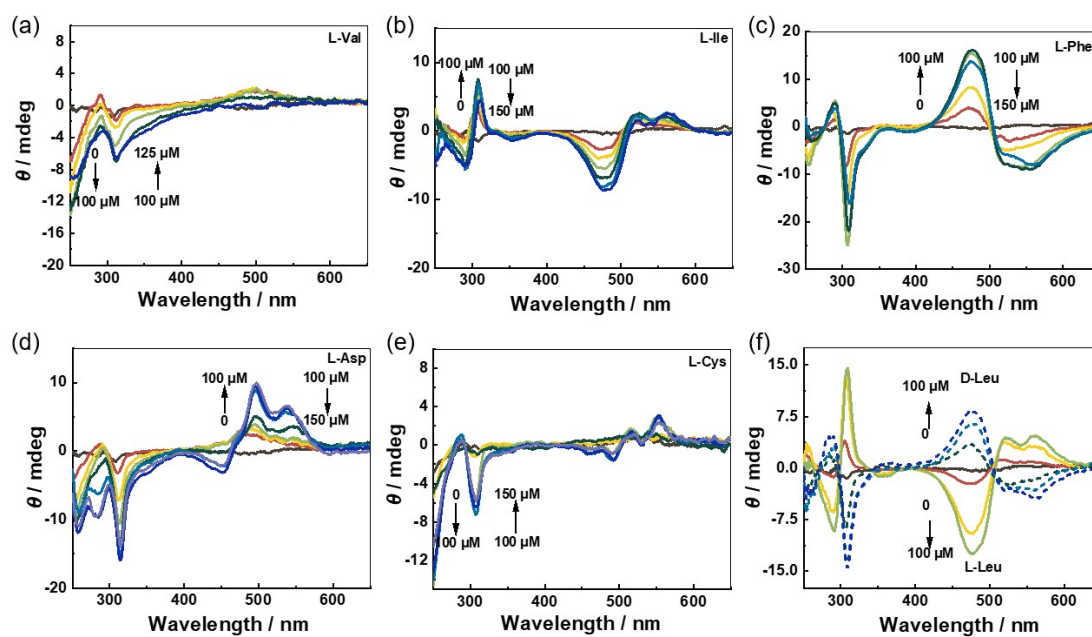


Fig. S21. CD spectra of S1 (0.05 mM) upon titration with (a) L-Val (0-125 μ M), (b) L-Ile (0-150 μ M), (c) L-Phe (0-150 μ M), (d) L-Asp (0-150 μ M), (e) L-Cys (0-150 μ M), (f) L/D-Leu (0-100 μ M) in 95% MCH at 25 $^{\circ}$ C.

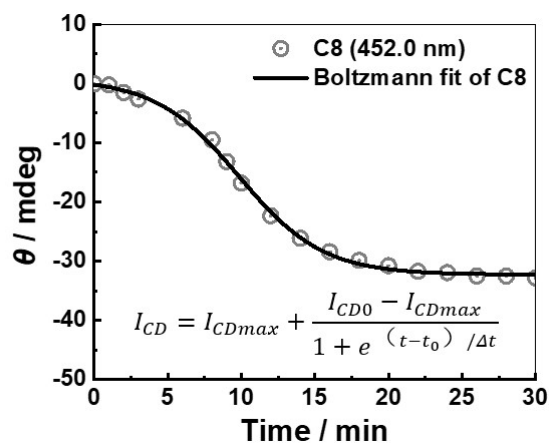


Fig. S22. Curve fitting for experimental points (gray circle) based on the Boltzmann equation of the formation kinetics of **Agg-C8** in 95% MCH at 25 °C. $[C8] = 0.05$ mM. I_{CD0} represent the CD intensities before aggregation and I_{CDmax} is the maximum CD intensities that aggregation reaching a stable state, t_0 is the time, in minutes, at which the inflection in CD intensity occurs, and Δt corresponds with the sigmoidal transition period as the CD intensity deviates from I_{CD0} in the semiloglinear regime, which is the reciprocal of the aggregation rate.

Table S2. Kinetic parameters of **Agg-C8** with L-Ser.^a

	t_0	Δt	R^2
C8	9.85 ± 0.141	2.85 ± 0.162	0.9985

^a data from Fig. S21.

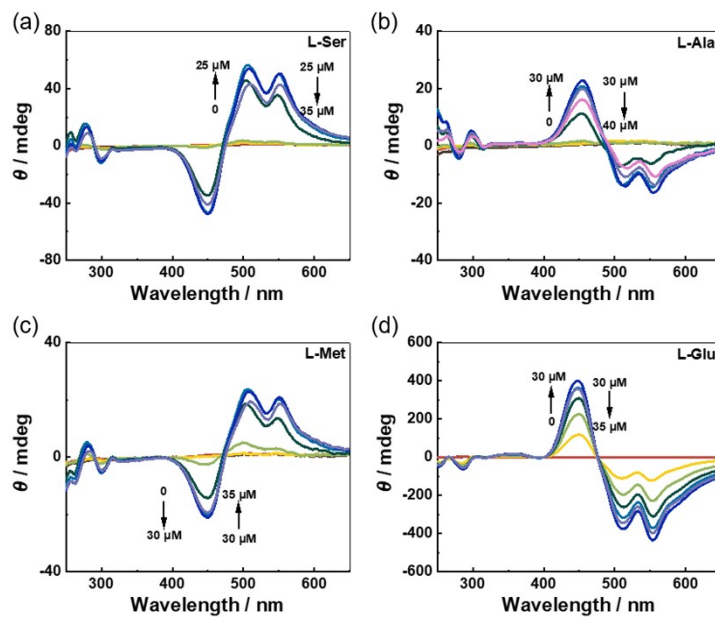


Fig. S23. CD spectra of **C8** (0.05 mM) upon titration with (a) L-Ser (0-35 μ M), (b) L-Ala (0-40 μ M), (c) L-Met (0-35 μ M), (d) L-Glu (0-35 μ M) in 95% MCH at 25 °C.

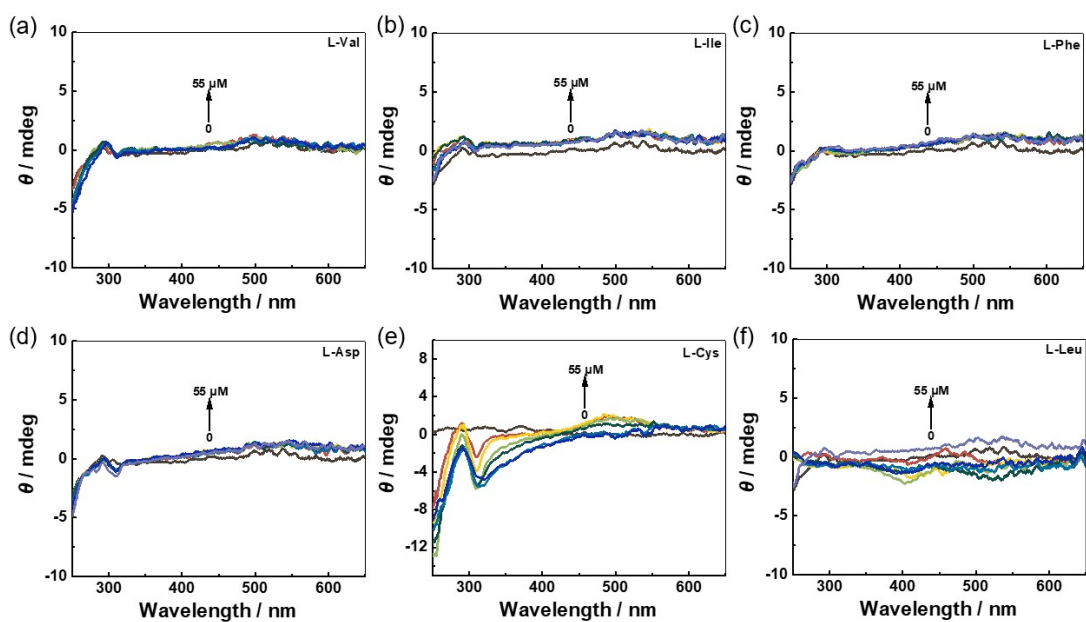


Fig. S24. CD spectra of C8 (0.05 mM) upon titration with (a) L-Val (0-55 μ M), (b) L-Ile (0-55 μ M), (c) L-Phe (0-55 μ M), (d) L-Asp (0-55 μ M), (e) L-Cys (0-55 μ M), (f) L-Leu (0-55 μ M) in 95% MCH at 25 $^{\circ}$ C.

- (1) (a) Zhao, T.; Yi, J.; Liu, C.; Liang, X.; Shen, Y.; Wei, L.; Xie, X.; Wu, W.; Yang, C., "First Come, First Served" and Threshold Effects in a Central-to-Planar-to-Helical Hierarchical Chiral Induction. *Angew. Chem. Int. Ed.* **2023**, *62*, e202302232; (b) Ji, J.; Li, Y.; Xiao, C.; Cheng, G.; Luo, K.; Gong, Q.; Zhou, D.; Chruma, J. J.; Wu, W.; Yang, C., Supramolecular enantiomeric and structural differentiation of amino acid derivatives with achiral pillar[5]arene homologs. *Chem. Commun.* **2020**, *56*, 161-164.